The Potential of Thermal Energy Storage for Sustainable Energy Supply at Chemical Sites

Marco Prenzel[1](✉), Freerk Klasing[1], Rüdiger Franck[2], Karen Perrey[3], Juliane Trautmann[4], Andreas Reimer[5], Stefan Kirschbaum[5], and Thomas Bauer[1]

[1] German Aerospace Center (DLR), Institute of Engineering Thermodynamics, 51147 Cologne, Germany
marco.prenzel@dlr.de
[2] Currenta GmbH & Co. OHG, Chempark, 51368 Leverkusen, Germany
[3] Covestro Deutschland AG, Chempark, 51365 Leverkusen, Germany
[4] TSK FLAGSOL Engineering GmbH, 50678 Cologne, Germany
[5] Gesellschaft zur Förderung Angewandter Informatik e. V, 12489 Berlin, Germany

Abstract. Ambitious greenhouse gas reduction targets and the currently surging energy prices pose significant challenges for the chemical industry. In this paper, the integration of molten salt thermal energy storage into the chemical site utility infrastructure is proposed to enable decarbonized and cost-effective electricity and process steam supply. The storage system is electrically charged and produces combined steam and electricity during discharge. A model of a utility infrastructure including all required input parameters was developed and implemented in the software Top-Energy® to perform operational optimizations and minimize operating costs. Simulation studies were carried out for different storage system configurations and the years 2020 to 2050. Attractive payback periods and net present values can be achieved with the described concept. Variable operating costs are largely reduced by the electrification of steam generation.

Keywords: Chemical Industry · Utility Infrastructure · Heat · Process Steam · Molten Salt · Optimized Operation · Decarbonization

1 Introduction

Many production processes in the chemical industry are energy-intensive and require a steady and reliable supply with large amounts of electricity and heat (mainly in the form of steam). To increase the efficiency of energy provision, centralized fossil fuel-fired cogeneration plants are typically employed at chemical sites [1]. As greenhouse gas reduction targets become more ambitious, the chemical industry must adapt existing utility infrastructures and operating strategies. German policy, for instance, calls for

The original version of this chapter was revised: The second reference citation [17] in the section 2.1.1 and consecutive reference citations have been corrected. The correction to this chapter is available at
https://doi.org/10.2991/978-94-6463-156-2_38

P. Schossig et al. (Eds.): IRES 2022, AHE 16, pp. 383–400, 2023.
https://doi.org/10.2991/978-94-6463-156-2_25

a 65% reduction in greenhouse gas emissions in 2030 compared to 1990 levels and carbon neutrality by 2045 [2]. Extended integration of renewable electricity from PV and wind with power-to-heat (PtH) is one key pathway to make the energy supply of the chemical industry net zero. Madeddu et al. investigated the CO_2 reduction potential in European industry using PtH [3]. The study showed that just from a technical point of view, about 78% of the industry's energy demand can be electrified with available technologies. On paper, electrification of up to 99% (excluding chemical feedstocks) is achievable if technologies currently under development, e.g. electric steam crackers [4], reach market maturity. However, the deployment of direct electrification is constrained by the availability and price volatility of renewable electricity. A switch to green hydrogen as a fuel for the cogeneration plants is also conceivable. The disadvantage of green hydrogen is its unpredictable price development, which may be as high as 159 €/MWh (based on the net calorific value) in 2050 [5], and the fact that considerable amounts of renewable electricity are needed for its production, as the overall efficiency is lower compared to direct electricity use.

Integrating a thermal energy storage (TES) system into the utility infrastructure of a chemical site can potentially be a building block to solve the abovementioned challenges and enable decarbonized and cost-effective electricity and heat supply. In this paper, integration of electro-thermal energy storage into the combined heat and power system (ETES-CHP) is proposed. The concept works as follows: During periods of high renewable electricity production, the TES system is electrically charged and the energy demand of the chemical site (heat and power) is met by electricity from the grid and, to the extent of available capacity, with PtH. When renewable electricity is in short supply, the TES system is discharged and produces steam directly in a molten salt steam generator and electricity via steam turbines, thus reducing the use of (renewable) fuels. Depending on the integration point and temperature level, different TES technologies can be applied. Viable options are regenerators, molten salt, phase change materials (PCM), Ruths steam accumulators and thermochemical energy storage (TCS). Klasing et al. provide an overview of the first four technologies and discuss readiness levels, advantages, and disadvantages [6]. The application of an electrically charged TCS system based on the reversable reaction of calcium oxide (CaO) and calcium hydroxide ($Ca(OH)_2$) was investigated by Backofen et al. [7, 8]. The storage system, consisting of two silos and two fluidized bed reactors [9], was integrated into an industrial heat and power plant model. The conducted operational optimizations showed that the TCS system improves the integration of electricity and thus reduces the operational expenditures (OPEX). Payback periods of under 10 years were reported for the considered use case. Garbrecht et al. performed process simulations of fossil power plants with integrated molten salt TES systems. It has been demonstrated that the use of a molten salt storage system can contribute to grid stability in two ways: (1) steadying the generator power output while meeting the customer's steam demand in a heat-controlled facility, (2) provision of control reserve in a power-controlled facility [10]. Bartsch and Zunft proposed the integration of TES (regenerator or molten salt) between the gas turbine and the downstream heat recovery steam generator (HRSG). Payback periods exceeded 10 years. This was attributed to the electricity and gas price curves considered and the particular configuration of the utility infrastructure. The available capacity of

the gas turbine was not sufficient during the winter months to simultaneously meet the steam demand and charge the storage unit [11]. A sodium nitrate ($NaNO_3$) PCM storage system has been successfully integrated into the steam line of a cogeneration plant in Germany, as reported by Johnson et al. Fuel consumption of existing backup boilers can be reduced because the PCM storage bridges the steam production while the backup boilers are ramping up. Hence, the backup steam generators must not be operated at minimal load [12, 13].

In general, the potential of TES in cogeneration plants as a flexibility option has been recognized. However, with the exception of Backofen et al. [7, 8], the aforementioned ETES-CHP concept has not been the focus of scientific studies. For this reason, the present paper elaborates on the application of the ETES-CHP concept with molten salt storage in utility infrastructures of large chemical sites. In particular, the following research subjects are addressed: (1) integration of the molten salt TES system into the utility infrastructure; (2) optimized operation to minimize OPEX; (3) evaluation methodology for TES integration concepts; (4) functionality of the storage concept; (5) quantifying economic benefits.

2 Applied Methods

The methods applied in this work are described in the following subsections.

2.1 Ideal-Typical Utility Infrastructure

An ideal-typical utility infrastructure (iUI) was previously introduced as a publicly available basis to investigate flexibility options for electricity and heat supply in the chemical industry [14]. The structure of the iUI is shown in Fig. 1. The iUI comprises three steam lines: high-pressure (HP, 110 bar and 530 °C), medium-pressure (MP, 31 bar and 370 °C) and low-pressure (LP, 6 bar and 210 °C). The temperature of LP and MP steam is lowered by water injection before it is delivered to customer's end-use processes. The steam specifications were adopted from the technical connection and delivery conditions of Currenta [15], an operator of chemical site utility infrastructures in Germany. The electricity demand of the end-use processes is largely covered from the local power grid. One gas turbine (GT), two back-pressure steam turbines (HP-ST and MP-ST) as well as one condensing turbine (LP-ST) serve as on-site power generators to reduce power purchase in periods of high electricity prices. Steam is produced by a three-stage HRSG connected to the GT, two large gas boilers (GB) and a small PtH unit. Small PtH units with double-digit MW output are increasingly used for steam generation in the chemical industry [16]. On the LP steam line, steam is extracted as required to preheat the feedwater for the GBs. Natural gas for the GT and GBs is obtained from the local gas grid. For more details on the iUI, especially component sizing, component efficiency and operation modes the reader is referred to the original publication [14].

2.1.1 Market Scenario

A market scenario for energy prices, CO_2 emission factors and CO_2 emission allowances is required for the calculation of energy costs. Electricity prices and average national electricity grid CO_2 emission factors should be available as hourly forward curves (HFC). For gas prices and CO_2 emission factors as well as CO_2 emission allowances, constant annual

values are sufficient. The market scenario used here is based on the European Green Deal [17] and was developed for the german energy system by the energy consultancy enervis energy advisors GmbH [18]. The key premises are as follows: (1) ongoing deployment of PV and wind power to ensure, inter alia, that electricity supply and consumption become carbon neutral before 2050 in accordance with the German Renewables Energy Act [19]; (2) nuclear phase-out by 2023 and coal phase-out by 2032; (3) continuous addition of green gases to the gas mix, switch to green hydrogen (0 t-CO_2/MWh) completed in 2045; (4) prices for CO_2 emission allowance increase according to the Sustainable Development Scenario of the World Energy Outlook 2020 [20]; (5) increased efficiency and refurbishment measures will reduce the overall heating demand by 25% until 2050, future heating demand will be covered through green gases as well as environmental (e.g. solar thermal), electric and district heating; (6) the increased use of electric vehicles reduces the energy demand in the transport sector by 50% until 2050, demand is divided approximately 50/50 between electric vehicles and synthetic fuels by the year 2050; (7) the required flexibilities are provided by pumped storage power plants, battery storage, electrolysers, load shedding and demand flexibility through e-mobility and the heating sector (heat pumps).

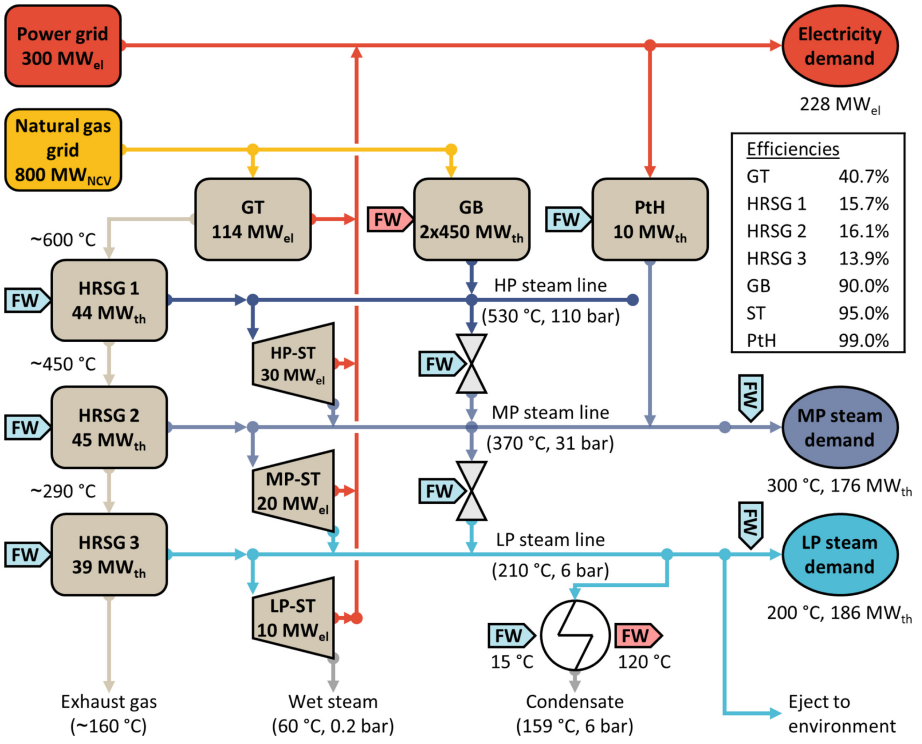

Fig. 1. Ideal-typical utility infrastructure, adapted from [14]. Abbreviations: FW: Feedwater, GB: Gas boiler, GT: Gas turbine, HP: High-pressure, HRSG: Heat recovery steam generator, LP: Low-pressure, MP: Medium-pressure, PtH: Power-to-heat, ST: Steam turbine

In the enervis market model, the three sectors electricity, heating and transport are modelled together with the transmission capacities to other countries. The optimal expansion path and operation of power plants, renewables, energy storage, etc. is determined in line with the given constraints. The development of average prices and emission factors for electricity and gas are illustrated in Fig. 2 a) and b), respectively. Historical market data is available for 2020, and data from 2021 to 2050 is obtained from the enervis market modelling. Electricity prices and average CO_2 emission factors of the national power grid have an hourly resolution (HFC). Constant annual values are available for gas. The cost of CO_2 emission allowances is included in the gas price (clean gas). The average price of electricity increases from 30 €/MWh to 74 €/MWh in the displayed 30-year span and peaks at 90 €/MWh in 2039. 90% of the electricity price values lie within the indicated 90% limits (the top and bottom 5% were discarded to improve readability). The 90% limits are to be understood as an indicator of the electricity price fluctuation. The fluctuations increase steadily up to 2040 and then remain largely unchanged until 2050. Starting in 2035, electricity prices around 0 €/MWh begin to occur more frequently. The clean gas price increases from 15 €/MWh to 74 €/MWh with a maximum of 81 €/MWh in 2044. Average CO_2 emission factors decrease almost steadily, starting at 0.373 tCO_2/MWh (electricity) and 0.201 tCO_2/MWh (gas), reaching 0 tCO_2/MWh in 2045. In 2030, the average CO_2 emission factor of electricity falls below that of gas. The main factor influencing iUI operation with and without a TES system, as will be shown later, is the electricity-to-clean-gas-price ratio:

$$R = \frac{c_{\mathrm{EL}}}{c_{\mathrm{CG}}} \tag{1}$$

c_{EL} and c_{CG} are the electricity and clean gas prices, respectively. Taxes and other expenses have not been considered in this work as they are site-dependant.

2.1.2 Other Input Parameters

The average electricity and total process steam demand as well as their basic course over a year were taken from [21]. Some changes were made, in particular hourly fluctuations were artificially added to better represent real load profiles. The magnitude of these fluctuations was adjusted to approximate real data, which was gratefully provided by Currenta. Further details can be found in [14]. For ambient temperature, data sets from the German Meteorological Service (Deutscher Wetterdienst) were used (Test Reference Year 2031–2060, Leverkusen Germany) [22].

2.2 Integration of Molten Salt TES

Two-tank molten salt TES is considered in this work because it is a commercial technology that is well established in the field of concentrated solar power (CSP) [23, 24]. The integration of the TES system into the iUI is illustrated in Fig. 3. Solar salt (60 wt.% $NaNO_3$ and 40 wt.% KNO_3) is used as a storage medium and heat transfer fluid. Three subsystems can be distinguished: (1) Storage unit: Solar salt is stored in a hot (565 °C) and a cold (274 °C) tank; (2) Charging unit: A pump conveys cold solar salt through an electric flow heater, which increases the temperature to the level of the hot

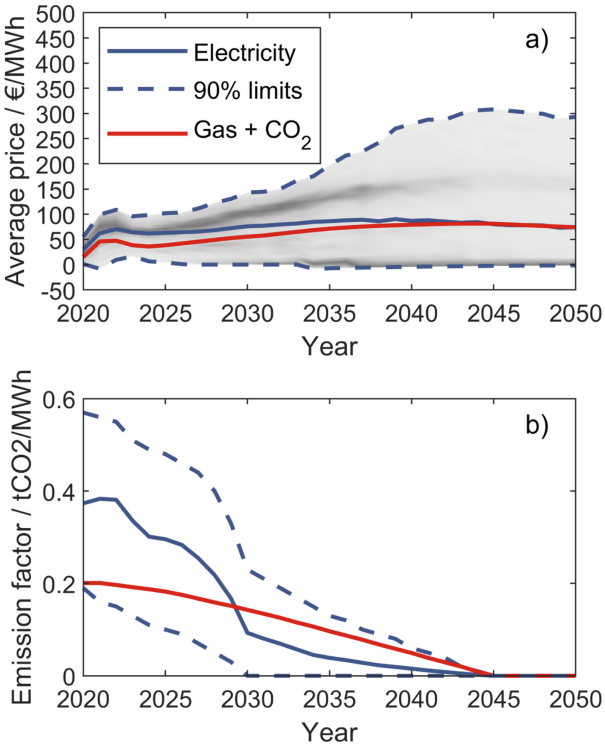

Fig. 2. Development of the average a) electricity and gas prices as well as b) CO_2 emission factors in the applied market scenario; values for gas are given with respect to the net calorific value; the greyscale in a) indicates how often a certain electricity price occurs (dark = often, light = less often).

tank; (3) Discharging unit: Hot solar salt is pumped through a molten salt steam generator producing high-pressure steam. Solar salt leaves the steam generator with the cold tank temperature. Similar to the GBs, feedwater preheating using low-pressure steam is required. The three subsystems can be sized and operated independently. By operating the charging and discharging units simultaneously, the storage system functions as a PtH unit that directly converts electricity from the grid into high-pressure steam. Larger dimensioning of the charging unit enables PtH operation with simultaneous charging of the storage unit. The presented integration concept is effectively the ETES-CHP system described in the introduction, as the available steam turbines of the iUI allow for power generation during discharge.

Basic engineering and cost estimation of the three subsystems were carried out by TSK Flagsol [25]. Heat losses amount to 1% of the total storage capacity per day. For confidentiality reasons, the derived cost functions cannot be disclosed in this paper.

2.3 Operational Optimization with Top-Energy® and Evaluation Methodology

The iUI with and without integrated molten salt TES was implemented in the software Top-Energy® version 2.11 [26]. Top-Energy® performs operational optimizations depending on the defined input (electricity price, clean gas price and temperature data) and output parameters (electricity and steam demand of the end-use processes). The optimization problem is expressed in an MILP (mixed integer linear programming) formulation. Top-Energy® solves the mathematical problem using the Gurobi solver [27].

The objective function is the minimum of annual variable operational expenditures:

$$\min\left\{OPEX_{\text{var}} = \sum (cQ)_{\text{CG,t}} + (cQ)_{\text{EL,t}}\right\} \tag{2}$$

The variable operational expenditures $OPEX_{\text{var}}$ are the sum of clean gas (CG) and electricity (EL) costs, which are the product of the price c and quantity Q of gas or electricity supplied from the grid at all time steps (t). Although operational optimization is carried out with respect to cost, Top-Energy® also calculates the CO_2 emissions associated with the use of gas and electricity for further evaluation. A rolling horizon algorithm with 1 h time steps, 24 h lookahead and 12 h writeback was applied [28].

The general evaluation methodology for TES integration concepts is outlined in Fig. 4. The iUI in its initial state (System A, as shown in Fig. 1) is used as a reference. Modifying the iUI by integrating a TES system results in System B (as depicted in Fig. 3). As already mentioned, the results of the operational optimization depend on the selected input parameters, shown on the left side in Fig. 4. These input parameters depend on the year or scenario considered. Energy price data, environmental data (temperature) and demand curves are input for the optimization with Top-Energy®. Further financial parameters are required for post-processing in order to calculate economic performance indicators. The variable operational expenditures determined with Top-Energy® are transferred to the economic analysis (post-processing). The use of a TES system provides the iUI with more flexibility for cheaper renewable power integration. For this reason, the variable operational expenditures of system B ($OPEX_{\text{B,var}}$) are reduced compared to system A ($OPEX_{\text{A,var}}$). Fixed operational expenditures ($OPEX_{\text{B,fixed}}$), due to additional maintenance (0,3% of the TES investment costs annually) and personnel (€150,000 annually), must be added to $OPEX_{\text{B,var}}$. A difference in operational expenditures between system A and B can then be calculated ($\Delta OPEX$). In addition, the investment costs of the TES unit ($\Delta CAPEX$) are required for the economic analysis. The discounted payback period (DPP) is determined as follows:

$$DPP = \ln\left(\frac{1}{1 - i\frac{\Delta Capex}{\Delta Opex}}\right) / \ln(1+i) \tag{3}$$

The interest rate i was fixed to 8% for this study [29, 30]. The net present value can be calculated from

$$NPV = -\Delta CAPEX + \sum_{t=1}^{n} \frac{\Delta OPEX_t}{(1+i)^t} \tag{4}$$

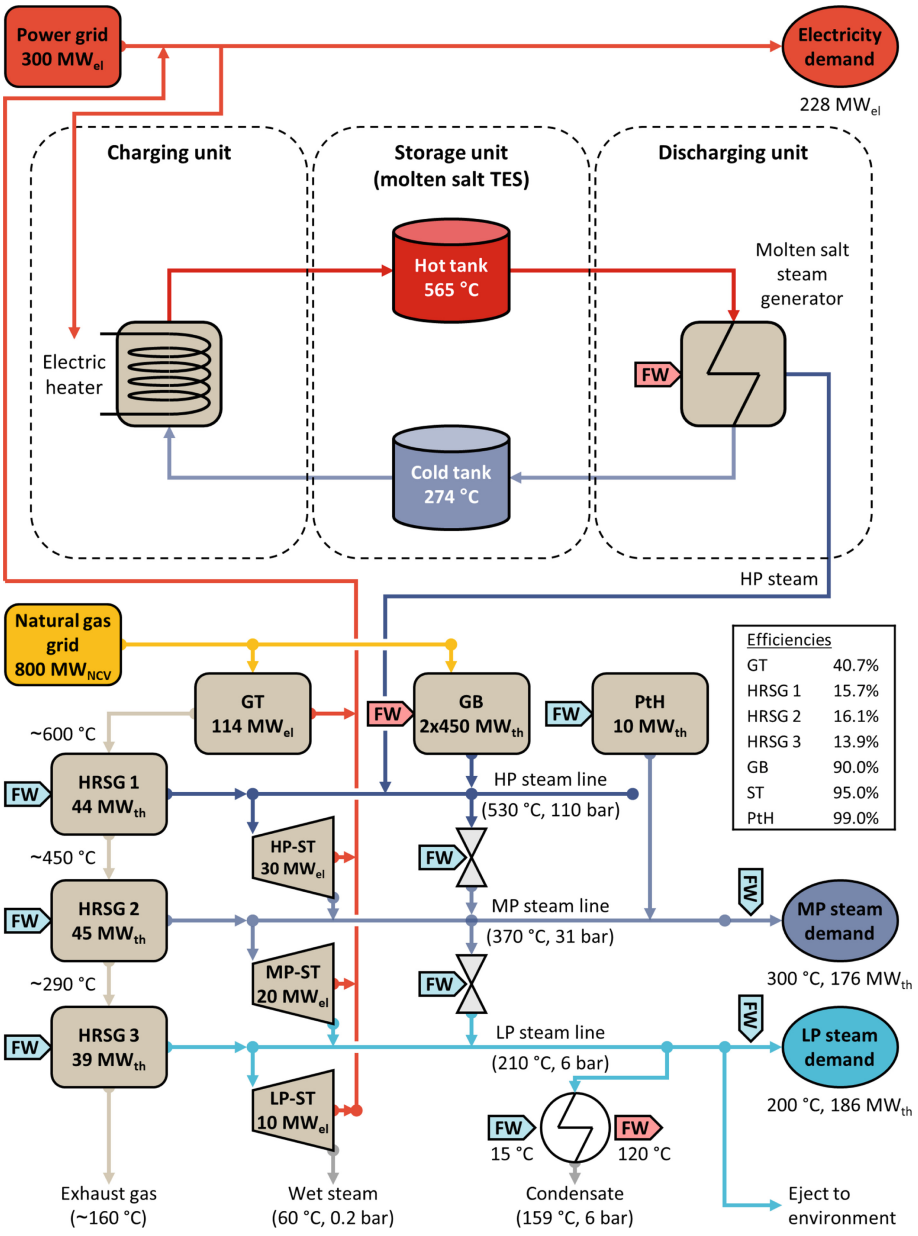

Fig. 3. Integration of molten salt TES into the ideal-typical utility infrastructure

with the year t and the financial lifetime of the TES system n. A value of 25 years was assumed for n [31]. Equation (3) is valid if $\Delta OPEX$ is determined for a single reference year and the value is then considered constant for the entire lifetime of the TES system. This applies to simulation runs with a single simulation year considered.

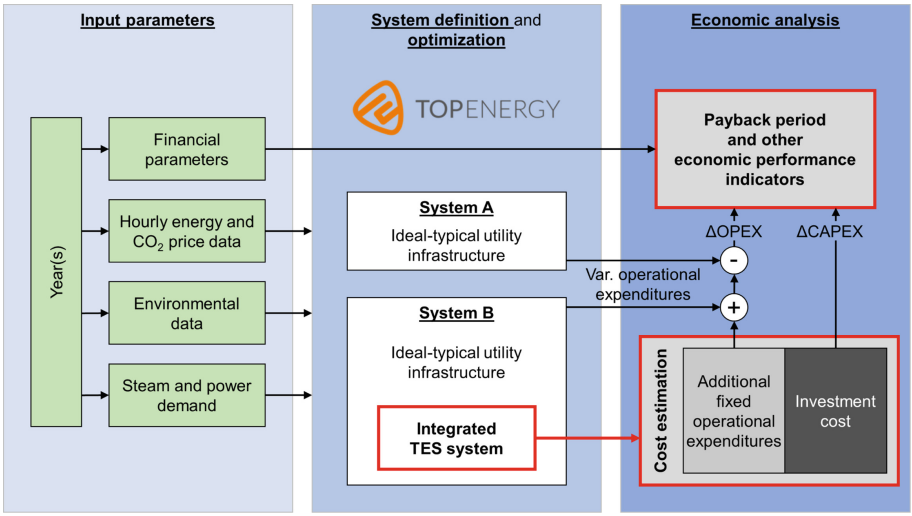

Fig. 4. General evaluation methodology for TES integration concepts in the iUI.

However, $\Delta OPEX$ may change over the years as electricity and clean gas prices vary. This is true for simulation runs over multiple years. In that case, the *DPP* was calculated manually. Changing $\Delta OPEX$ are already considered in Eq. (4) through the index t.

2.4 Conducted Simulations

A total of three simulation studies were conducted. In the first study, an operational optimization was performed for an exemplary TES system and the year 2045 (first year with 0 tCO_2/MWh emission factors). To this end, a TES system with 500 MW charging, 3000 MWh storage and 250 MW discharging unit was selected. The results obtained were analysed in detail. Based on this example, the TES operation strategy and its main influencing factors are determined. In addition, the results should provide insight on how the deployment of the ETES-CHP system changes the electricity and steam supply of the iUI.

In the second study, the dimensions of the TES system (size of the charging, storage and discharging unit) were varied. Due to the large number of permutations, again only 2045 was considered as the simulation year. The variation of the size of the three subsystems is summarized in Table 1.

For the power units, the charging/discharging duration in hours was defined instead of a MW-value to ensure that their size was always consistent with the storage capacity considered. First, all possible combinations of charging, storage and discharging units were compiled. From a total of 175 (5 x 7 x 5) possible combinations, the ones with discharging unit > charging unit were then filtered out, as these were determined to be uneconomical in preliminary studies. In addition, all unit dimensions were checked to see if they were within the used cost functions and adjusted if required. In the end, 94 different storage systems were evaluated.

Table 1. Variation of the TES subsystems

Subsystem	Duration/Sizes
Charging unit	[1, 6, 12, 18, 24] h
Storage unit	[50, 100, 250, 500, [1000, 3000, [5500] MWh
Discharging unit	[1, 6, 12, 18, 24] h

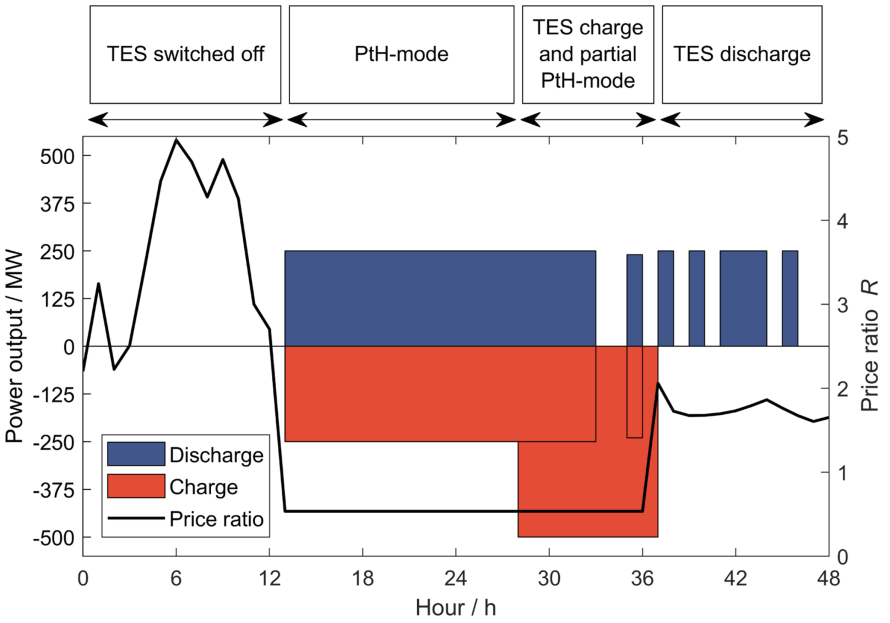

Fig. 5. Operating strategy of the TES system in response to the electricity-to-clean-gas-price ratio during two sample days in 2045; TES system with 500 MW charging, 3000 MWh storage and 250 MW discharging unit.

In the third and final study, a continuous operational optimization was carried out for the period 2020–2050, using the corresponding market scenario prices for each individual year. The objective of this study is to identify the point at which year the deployment of an ETES-CHP system in the iUI can provide a financial benefit. To this end, the TES system from the first study with 500 MW charging, 3000 MWh storage and 250 MW discharging unit was again selected as an example.

3 Results and Discussion

According to the three studies conducted, the results section is divided into three subsections. The operating strategy of the TES system is subject of the first subsection (Study 1). Then, the results of the TES size variation are presented (Study 2). Finally, the operational optimization over the entire time frame of the market scenario from 2020–2050 is discussed (Study 3).

3.1 TES Operating Strategy (Study 1)

Analysis of the optimization results showed that the operating strategy of a TES system depends primarily on the electricity-to-clean-gas-price ratio *R*. To illustrate this, Fig. 5 shows the power output of the discharging (positive values) and charging (negative values) unit as well as the price ratio *R* over two sample days in 2045. In the first 12 h the price ratio is well above a value of 2, which means that electricity is more than twice as expensive as gas. In this case, the iUI employs its gas-fired steam generators while the GT and STs run at full load to minimize the amount of electricity procured from the grid. The TES system is not utilized in this case. In the following hours *R* drops below a value of 1 and the TES system switches to PtH mode. Charging and discharging unit are operated simultaneously and with the same power to directly convert electricity into steam. In such instances the GT and STs are shut down and the GBs supply the remaining steam required to cover the demand. At approximately 36 h, the price ratio *R* increases again. In the hours before this point, the charging unit is ramped up to maximum capacity to charge the storage unit.

In some hours, the discharging unit is still in operation, i.e. PtH operation and storage charging occur simultaneously. After the sharp increase of the price ratio at 36 h, the charging unit is switched off and the storage unit is discharged. In this way, the price fluctuations on the electricity market are exploited to lower the variable OPEX of the iUI (charge and discharge mode).

With increased PtH capacity and the ability to take advantage of price fluctuations on the energy market, the TES unit changes the operation strategy of the iUI and thus the manner in which the electricity and steam demand of the end-use processes is met. This effect is highlighted in Fig. 6. The electricity demand coverage in the year 2045 is shown on the left-hand side. Figure 6-a depicts the electricity supply of the iUI in its initial state. The electricity demand coverage of the iUI with an integrated TES system (500 MW charging, 3000 MWh storage and 250 MW discharging unit) is displayed in Fig. 6-b. It can be seen that due to the limited power generation capacity of the iUI, a large amount of electricity must be procured from the grid. This applies regardless of the availability of a TES unit. The remaining electricity demand is met by the GT and the available STs. Without a TES system, the STs are powered by steam exclusively from the gas-fired GBs or the HRSG. The integrated TES system substitutes about 2/3 of the steam usage of the STs. This is due to the charge and discharge mode outlined in Fig. 5, where the TES system is charged at low electricity-to-clean-gas-price ratios to be discharged again after a sharp price increase. The coverage of the steam demand in the year 2045 is shown on the right-hand-side in Fig. 6. Figure 6-c depicts the case with the iUI in the initial state and Fig. 6-d with integrated TES. It is evident that the influence

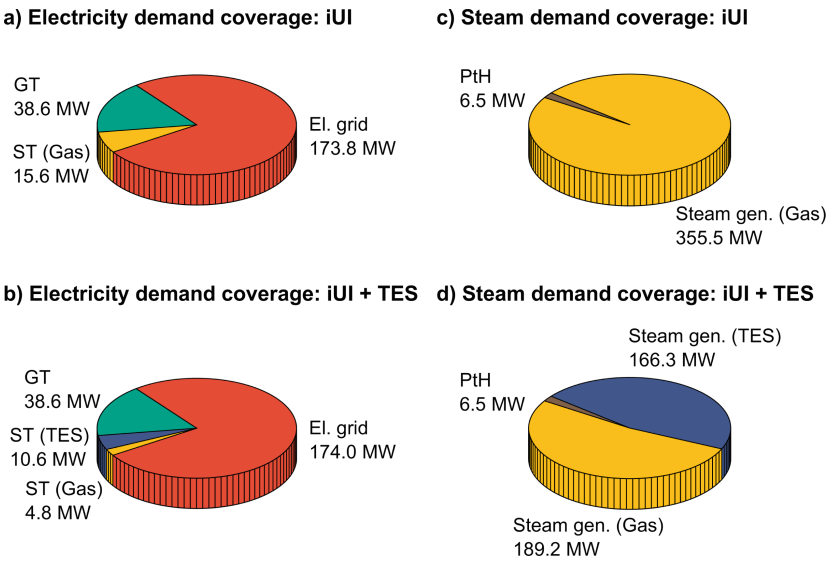

Fig. 6. Electricity demand supplied by the a) iUI or b) iUI + TES (left); and steam demand supplied by the c) iUI or d) iUI + TES (right) in the year 2045; TES system with 500 MW charging, 3000 MWh storage and 250 MW discharging unit. Abbreviations:ST (Gas): Steam turbine output with steam from gas-fired components, ST (TES): Steam turbine output with steam from TES, Steam gen. (Gas): Steam supplied by gas-fired components, Steam gen. (TES): Steam supplied by TES.

of the TES system is more pronounced on the steam supply side. In its initial state, the iUI generates steam almost exclusively with the gas-fired GBs and the HRSG. Less than 2% of the steam demand can be covered by the existing small PtH unit. With the TES system, the steam generation is electrified to a significantly greater extent (almost 50%). Key to the increased steam electrification is the PtH function of the TES system at low price ratios. After detailed analysis of the results data, it was identified that the most relevant factors influencing the impact of the TES system are: (1) size of the storage, charge and discharge units; (2) number of hours per year with favourable price-ratios R for PtH operation; (3) frequency and magnitude of fluctuations in the price ratio R; (4) size of the available STs compared to the electricity demand.

3.2 TES Size Variation (Study 2)

To examine the influence of TES system size, Fig. 7 shows the result of the second simulation study and plots the net present value (NPV) versus the discounted payback period (DPP) for all TES configurations considered. The x-axis was restricted to discounted payback periods less than 10 years, since TES systems with $DPP > 10$ a are not economically relevant. The most economical TES systems have a short DPP and achieve a high NPV after their 25-year financial lifetime. Few of the smaller storage systems of 50 or 100 MWh can achieve competitive payback periods and the net present values are limited due to the high specific costs of these small systems. A TES system

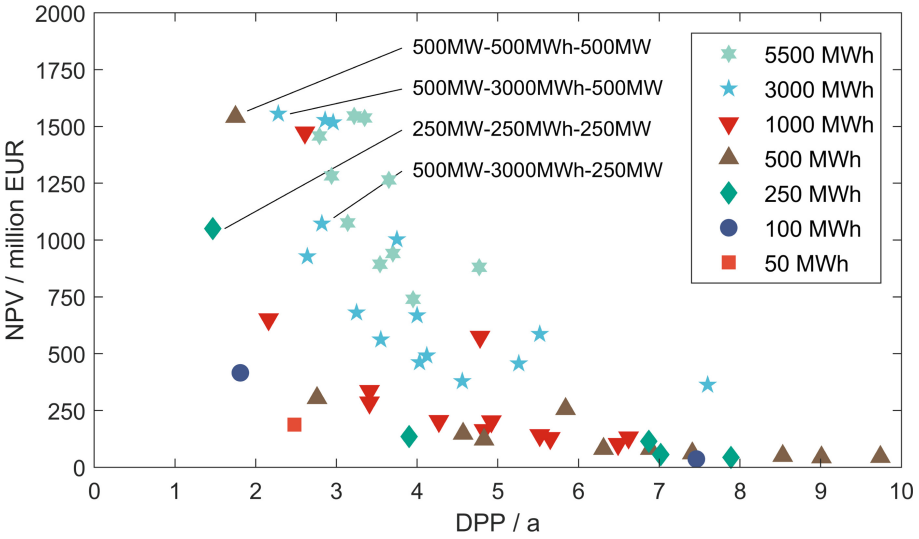

Fig. 7. Net present value *NPV* over discounted payback period *DPP* for all TES configurations and the year 2045.

with 250 MW charging, 250 MWh storage and 250 MW discharging unit achieves the shortest *DPP* with 1.5 years. This particular system is large enough to take advantage of economies of scale. The reduction in variable operating costs is achieved mainly through PtH functionality. The 250 MW capacity ensures that the system's output can be fully utilized at any hour of the year, as the average steam demand is 362 MW. A similar and larger system with 500MW-500MWh-500MW achieves a significantly higher *NPV* of €1.54 billion compared to €1.05 billion, while the *DPP* increases to 1.8 years. Improved economies of scale and enhanced electrification of steam demand benefit the net present value. However, 500 MW exceeds the value of the average steam demand, which means that the TES system cannot always be operated at full load. This leads to a slightly higher discounted payback period. A TES system with 500MW-3000MWh-500MW achieves the highest *NPV* of €1.57 billion with a *DPP* of 2.3 years. However, the difference in net present value compared to the 500MW-500MWh-500MW system is only marginal. While both TES systems have the same PtH capacity, the larger storage unit should result in an improved exploitation of price ratio fluctuations. Since the monetary effect of charging and discharging energy appears to be limited, it can be concluded that the market scenario considered does not display sufficient price ratio fluctuations in terms of frequency and amplitude to make larger storage capacities profitable. Higher steam turbine capacity resulting in a higher power to power efficiency may also be favourable to take advantage of the charge and discharge mode.

3.3 Operational Optimization from 2020 to 2050 (Study 3)

The results of the third simulation study in terms of annual OPEX and cumulative CO_2 emissions are shown in Fig. 8 a) and b), respectively. Because of increased electricity

and gas prices, the annual OPEX of the iUI almost quadruple, from €97 million in 2020 to €365 million in 2050. Annual OPEX peak in 2041 at €413 million.

This development can be counteracted with the proposed ETES-CHP system. In 2050 for instance, deployment of a 500MW-3000MWh-250MW TES system reduces the annual OPEX from €365 to €246 million. Study 1 and 2 assumed constant OPEX savings over the financial lifetime of the TES system. In this study, it becomes clear that variable OPEX change over the years. Therefore, the year of installation of the TES system is relevant to its economic feasibility. In this case, a $DPP < 3$ years can only be achieved if the TES system is deployed after 2043. However, a $DPP < 5$ years can be realized as early as 2034. Therefore, it may be advantageous to install a TES system earlier to reduce variable OPEX, at the cost of a moderately higher DPP. In addition, the use of the TES system can reduce total cumulative CO_2 emissions from 2020 to 2050 by up to 3 Mt (21%). This is only a side effect of operational optimization, as more low-cost electricity with a low CO_2 emission factor is utilized for steam generation. It can be expected that optimizing operations to minimize CO_2 emissions (compared to an economic optimization as shown in Fig. 8) will lead to even more substantial greenhouse gas reductions.

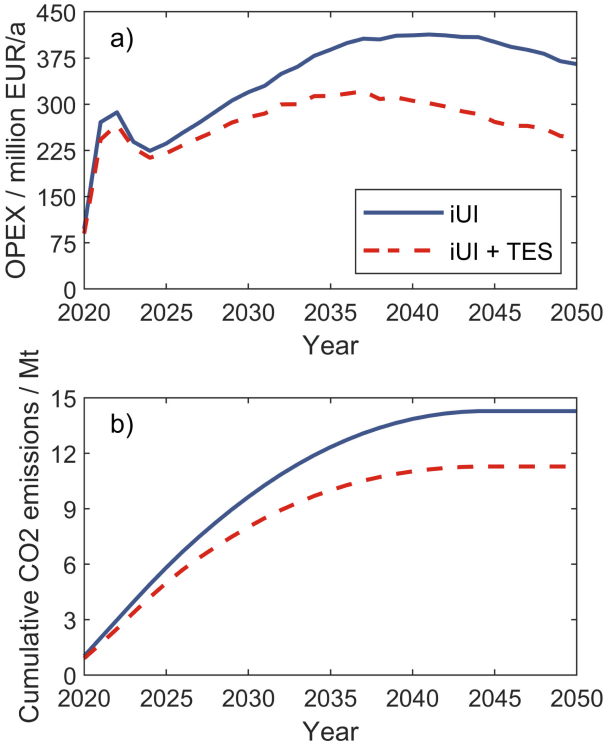

Fig. 8. Development of the a) annual OPEX and b) cumulative CO_2 emissions from 2020 to 2050 with and without a 500MW-3000MWh-250MW TES system.

4 Conclusions and Outlook

In this work, the use of a molten salt based electro-thermal energy storage with combined heat and power system (ETES-CHP) in a chemical site utility infrastructure was investigated. For this purpose, a so-called ideal-typical utility infrastructure (iUI) was implemented in the optimization software TOP-Energy®. A market scenario based on the European Green Deal was considered. In this market scenario, the maximum price for green hydrogen is €81/MWh. This represents a moderate increase compared to other price prognoses (159 €/MWh [5]) or current gas prices of 2022. Three studies were carried out: (1) Operational optimization of an exemplary TES system in 2045 to assess the operation strategy and influencing factors; (2) Size variation of the charging, storage and discharge unit in the year 2045 to determine potential discounted payback periods and net present values; (3) Evaluation of a single TES system from 2020–2050 to identify feasible installation years and determine overall CO_2 reduction potentials.

The first study showed that the TES system integrates low-cost electricity in two ways: (1) PtH mode: Direct steam generation via PtH when the electricity price is low compared to that of clean gas, (2) Charge and discharge mode: Exploiting price fluctuations by storing electricity in the form of thermal energy and discharging after a sharp price increase. As a result, the available steam turbines are increasingly driven by steam generated with the TES unit and a large proportion of the steam supply is electrified. The second study illustrated that under the selected boundary conditions, TES systems can achieve short payback periods in the range of few years and high net present values, depending on the configuration (size of the charging, storage and discharging unit). The PtH mode is the decisive factor for these positive results. With the utilized scenario with a relatively low (CO_2 free) gas price (€81/MWh maximum), the number and amplitude of electricity price fluctuations are not sufficient for the charge and discharge mode to have a significant overall impact through electricity arbitrage alone. Finally, the third study highlighted that the proposed ETES-CHP concept can achieve competitive payback periods of < 5 years when deployed as early as 2034 and total CO_2 emissions (from 2020–2050) can be reduced by up to 21%.

A deeper understanding of the sensitivities requires further studies. In particular, different market scenarios (e.g. higher gas prices) and a modification of the iUI (e.g. larger steam turbines) may have a positive effect on the performance and functionality of the ETES-CHP concept. Based on the results, a comparison with other PtH technologies (electrode boilers, immersion heaters or heat pumps) is also a logical next step.

Acknowledgments. The authors thank the German Federal Ministry for Economic Affairs and Climate Action (BMWK) for the financial support given to this work in the project TransTES-Chem 03ET1646A-E.

Authors' Contributions. **Marco Prenzel**: Conceptualization, Methodology, Formal analysis, Data Curation, Writing - Original Draft, Visualization **Freerk Klasing**: Writing - Review & Editing **Rüdiger Franck**: Resources, Writing - Review & Editing **Karen Perrey**: Funding acquisition **Juliane Trautmann**: Resources, Writing - Review & Editing **Andreas Reimer**: Software, Formal analysis, Data curation **Stefan Kirschbaum**: Software, Funding acquisition **Thomas Bauer**: Methodology, Supervision, Project administration, Funding acquisition, Writing - Review & Editing.

References

1. United Nations Industrial Development Organization, Manual for industrial steam systems assessment and optimization, 2016: Available: https://www.unido.org/sites/default/files/2017-11/SSO-Manual-Print-FINAL-20161109-One-Page-V2.pdf (accessed July 18 2022)
2. German Federal Ministry for the Environment, Nature Conservation, Nuclear Safety and Consumer Protection, Revised Climate Change Act sets out binding trajectory towards climate neutrality by 2045. Available: https://www.bmuv.de/PM9586-1 (accessed July 18 2022)
3. S. Maddedu, F. Ueckerdt, M. Pehl, et al., The CO2 reduction potential for the European industry via direct electrification of heat supply (power-to-heat), Environmental Research Letters, vol. 15, 2020, 124004. DOI: https://doi.org/10.1088/1748-9326/abbd02
4. S.T. Wismann, J.S. Engbæk, S.B. Vendelbo, et al., Electrified methane reforming:A compact approach to greener industrial hydrogen production, Science, vol. 364, issue 6442, 2019. pp. 756–759. DOI: https://doi.org/10.1126/science.aaw8775
5. M. Robinius, P. Markewitz, P. Lopion, et al., Wege für die Energiewende - Kosteneffiziente und klimagerechte Transformationsstrategien für das deutsche Energiesystem bis zum Jahr 2050, Schriften des Forschungszentrums Jülich, Energy & Environment, vol. 499, 2020. Available: https://juser.fz-juelich.de/record/877960/files/fEnergie_Umwelt_499.pdf (accessed July 18 2022)
6. F. Klasing, C. Odenthal, T. Bauer, Assessment for the adaptation of industrial combined heat and power for chemical parks towards renewable energy integration using high-temperature TES, Energy Procedia, vol. 155, 2018, pp. 492-502. DOI: https://doi.org/10.1016/j.egypro.2018.11.031
7. G. Backofen, M. Würth, A. Vandersickel, et al., Power-to-Process-Heat in Industrial Combined Heat and Power Plants – Integration of a Large-Scale Thermochemical Energy Storage, Proceedings of the International Renewable Energy Storage Conference 2021 (IRES 2021), pp. 8–17. DOI: https://doi.org/10.2991/ahe.k.220301.002
8. G. Backofen, J. Haimerl, A. Vandersickel, et al., Thermochemical Energy Storage for Increasing the Flexibility of an Industrial Combined Heat and Power Plant, Proceedings of the 34th International Conference on Efficiency, Cost, Optimization, Simulation and Environment Impact of Energy Systems, 2022, pp. 1074–1085. DOI: https://doi.org/10.52202/062738-0095
9. M. Angerer, M. Becker, S. Härzschel, et al., Design of a MW-scale thermo-chemical energy storage reactor, Energy Reports, vol. 4, 2018, pp. 507-519. DOI: https://doi.org/10.1016/j.egyr.2018.07.005
10. O. Garbrecht, M. Bieber, R. Kneer, Increasing fossil power plant flexibility by integrating molten-salt thermal storage, Energy, vol. 118, 2017, pp. 876-883. DOI: https://doi.org/10.1016/j.energy.2016.10.108

11. P. Bartsch, S. Zunft, Thermische Energiespeicher, in: F. Ausfelder, S. von Roon, A. Seitz (Eds.), Flexibilitätsoptionen in der Grundstoffindustrie II, 2019, Available: https://dechema.de/dechema_media/Downloads/Positionspapiere/2019_Kopernikus_Flexoptionen_Band+II_kompl.pdf (accessed July 18 2022)
12. M. Johnson, A. Dengel, B. Hachmann, et al., Integration of a latent heat storage unit in a cogeneration plant, Proceedings of the International Sustainable Energy Conference 2018. Available: https://elib.dlr.de/122209/1/Johnson_Abstract.pdf (accessed July 18 2022)
13. M. Johnson, M. Fiß, A. Dengel, et al., Commissioning of high temperature thermal energy storage for high power levels, Proceeding of the conference Enerstock 2021. Available: https://elib.dlr.de/147147/1/IEA-ECES_TESIN.pdf (accessed July 18 2022)
14. T. Bauer, M. Prenzel, F. Klasing, et al. Ideal-Typical Utility Infrastructure at Chemical Sites – Definition, Operation and Defossilization, Chemie Ingenieur Technik, vol. 94, issue 6, 2022, pp. 840-851. DOI: https://doi.org/10.1002/cite.202100164
15. CURRENTA GmbH & Co. OHG, Technische Anschluss- und Lieferbedingungen für den Anschluss an die Energieversorgungsnetze der CURRENTA GmbH & Co. OHG, 2007: Available: https://energie.currenta.de/media/dokumente/TALB.pdf (accessed July 18 2022)
16. CURRENTA GmbH & Co. OHG, Neuer Kessel für stabile Netze und grünen Strom, 2020. Available: https://www.currenta.de/medien/presseserver/presseserver-news/items/2020-07-24-neuer-kessel-fuer-stabile-netze-und-gruenen-strom.html (accessed July 18 2022)
17. European Commission, A European Green Deal - Striving to be the first climate-neutral continent. Available: https://ec.europa.eu/info/strategy/priorities-2019-2024/european-green-deal_en (accessed July 18 2022)
18. enervis energy advisors GmbH. Available: https://enervis.de/en/about-us/ (accessed July 18 2022)
19. International Energy Agency (IEA), Germany's Renewables Energy Act. Available: https://www.iea.org/policies/12392-germanys-renewables-energy-act (accessed July 18 2022)
20. International Energy Agency (IEA), World Energy Outlook 2020. Available: https://www.iea.org/reports/world-energy-outlook-2020 (accessed July 18 2022)
21. F. Ausfelder, C. Beilmann, M. Bertau, et al., Energy Storage Technologies as Options to a Secure Energy Supply, Chemie Ingenieur Technik, vol. 87, issue 1–2, 2015, pp. 17–89. DOI: https://doi.org/10.1002/cite.201400183
22. German Meteorological Service (Deutscher Wetterdienst), Testreferenzjahre (TRY). Available: https://www.dwd.de/DE/leistungen/testreferenzjahre/testreferenzjahre.html (accessed July 18 2022)
23. T. Bauer, C. Odenthal, A. Bonk, Molten Salt Storage for Power Generation, Chemie Ingenieur Technik, vol. 93, issue 4, 2021, pp. 534-546. DOI: https://doi.org/10.1002/cite.202000137
24. Md.T. Islam, N. Huda, A.B. Abdullah, et al., A comprehensive review of state-of-the-art concentrating solar power (CSP) technologies: Current status and research trends, Renewable and Sustainable Energy Reviews, vol. 91, 2018, pp. 987-1018. DOI: https://doi.org/10.1016/j.rser.2018.04.097
25. TSK Flagsol. Available: https://www.grupotsk.com/en/ (accessed July 18 2022)
26. The Society for the Advancement of Applied Computer Science, Top-Energy Version 2.11. Available: https://www.top-energy.de/en (accessed July 18 2022)
27. Gurobi, Gurobi Optimizer. Available: https://www.gurobi.com/products/gurobi-optimizer/ (accessed July 18 2022)
28. Advanced Interactive Multidimensional Modeling System (AIMMS), Implementing a Model with a Rolling Horizon. Available: https://documentation.aimms.com/language-reference/advanced-language-components/time-based-modeling/implementing-a-model-with-a-rolling-horizon.html (accessed July 18 2022)

29. V. Jülch, Comparison of electricity storage options using levelized cost of storage (LCOS) method, Applied Energy, vol. 183, 2016, pp. 1594-1606. DOI: https://doi.org/10.1016/j.apenergy.2016.08.165
30. A. Smallbone, V. Jülch, R. Wardle, et al., Levelised Cost of Storage for Pumped Heat Energy Storage in comparison with other energy storage technologies, Energy Conversion and Management, vol. 152, 2017, pp. 221–228. DOI: https://doi.org/10.1016/j.enconman.2017.09.047
31. IRENA (2020), Innovation Outlook: Thermal Energy Storage, International Renewable Energy Agency, Abu Dhabi. Available: https://www.irena.org/publicationsearch?keywords=Thermal%20energy%20storage (accessed July 18 2022)